

Impact of Tracker Design on Higgs Mass and Cross Section

Hai-Jun Yang Keith Riles*

Department of Physics, University of Michigan, Ann Arbor, MI 48109-1120, USA

(Dated: August 14, 2002)

We have studied the impact of charged track resolution on Higgs mass and production cross section measurement in the process $e^+e^- \rightarrow Z^0 H, Z^0 \rightarrow \ell^+\ell^-, H \rightarrow X$ for Higgs masses between 120 and 160 GeV, assuming the Next Linear Collider(NLC) is operated at 350 GeV and 500 GeV center of mass energies with integrated luminosities of 500 fb^{-1} . Using fast and full Monte Carlo simulations of the 2001 North American baseline detector designs (LD and SD), we confirm that the Higgs mass resolution is only sensitive to degraded momentum resolution, but less sensitive to improved momentum resolution and track angular resolution. The cross section resolution and hence absolute branching fraction resolution are insensitive to angular and momentum resolutions. The SD detector provides a more accurate measurement than the LD of the Higgs mass.

I. INTRODUCTION

To illustrate why it is premature to carry out these studies using full Monte Carlo simulation, we show comparison of track momentum resolution in FIG. 1 and fractional momentum resolution in FIG. 2 for the LD and SD detector baselines. The solid curves show expected resolutions from an analytic approach [1], and the dots show resolutions determined for different polar angle regions for fast and full Monte Carlo simulation of samples of 100K tracks in hadronic background events. While the fast Monte Carlo simulation results are in good agreement with expectation, the full Monte Carlo simulation, including track reconstruction, is clearly far from optimum.

II. ANALYSIS

The Higgs mass can be simply determined assuming recoil in the process $e^+e^- \rightarrow Z^0 H, Z^0 \rightarrow \ell^+\ell^-, H \rightarrow X$ ($\ell = e, \mu$). The recoil mass is defined as:

$$M_H^{recoil} = \sqrt{s - 2\sqrt{s} \cdot E_{\ell^+\ell^-} + M_{\ell^+\ell^-}^2}$$

where s is the center-of-mass energy squared, $E_{\ell^+\ell^-}$ is the energy of the lepton pair from Z^0 decay, while $M_{\ell^+\ell^-}$ is the pair's invariant mass. The main backgrounds of this analysis are $e^+e^- \rightarrow Z^0 Z^0, W^+W^-$, but other sources of contamination, including Bhabha events, dimuon and two photons events are also investigated.

Monte Carlo events in this analysis were generated by the Pandora(V2.2)-Pythia(V3.1) package [2, 3] which includes initial state radiation, beamsstrahlung, beam energy spread(full width is 1%), hadron fragmentation and final state QCD/QED radiation. In addition, the electron beam is polarized to -80% . The Java Analysis Studio(JAS) [4] package was used to analyze fast and full detector simulation events, assuming the LD and SD baseline detectors [1, 5, 6].

These studies are performed for a Next Linear Collider operated at center-of-mass energies of 350 GeV and 500 GeV with integrated luminosities of 500 fb^{-1} each, assuming Higgs mass between 120 and 160 GeV. Events are selected using a cut-based approach, according to the following criteria [7]:

- (1) A candidate lepton must have an energy greater than 10 GeV
- (2) The polar angle of a lepton must satisfy $|\cos\theta_e| < 0.9$
- (3) There must be at least 2 lepton candidates in the event
- (4) The invariant mass of the lepton pair must lie within 5 GeV of the Z^0 mass
- (5) The polar angle of two-lepton system must lie in the barrel region, $|\cos\theta_{e^+e^-}| < 0.6$
- (6) The opening angle between the two leptons should satisfy $|\cos\theta_{e^+\leftrightarrow e^-}| > -0.7$

*Electronic address: yhj@umich.edu, kriles@umich.edu

Cut (5) is used to suppress $Z^0 Z^0$ background, while Cut (6) reject background from W^+W^- . The selection efficiency for signal is about 48-50% for 350 GeV center-of-mass energy listed in TABLE I. The signal efficiency is higher, 55-56%, at a 500 GeV machine, mainly because the higher Lorentz boost of the leptons from Z^0 decay leads to a smaller average opening angle. For full SD events, however, the selection efficiency degrades 6-8% because of low track reconstruction efficiency in SD forward region.

\sqrt{s}	m_{higgs}	Eff. of fast MC		Eff. of full MC	
(GeV)	(GeV)	LD(%)	SD(%)	LD(%)	SD(%)
500	120	55.2	55.2	55.5	49.7
	140	55.4	55.4	55.9	49.6
	160	55.2	55.3	56.8	50.4
350	120	49.9	50.0	48.2	41.2
	140	48.2	48.2	48.6	40.8
	160	48.0	47.9	47.6	38.7

TABLE I: Selection efficiencies of $e^+e^- \rightarrow ZH \rightarrow \mu^+\mu^- X$ for two baseline detectors, assuming NLC is operated at 350 and 500 GeV center of mass energies with Higgs masses between 120 and 160 GeV.

Beam energy spread with full width 1%, included in new version of Pandora(V2.2), makes Z recoil mass distribution much wider than that from without beam energy spread. The comparison is shown in FIG. 3.

For the full detector simulation MC, the recoil mass distributions are a little worse than that from fast MC, shown in FIG. 4. Here, we use default beam setup(NLC500H) for $\sqrt{s} = 500$ GeV. Large discrepancy between recoil mass spectra of fast and full MC is seen for silicon detector. It's not surprising because the track reconstruction efficiency is quite low in SD forward region which eventually results in low selection efficiency.

III. COMPARISON AND CONCLUSION

In order to investigate the dependence of Z recoil mass distribution on track momentum resolution, we re-scale track resolution by factor from 0.25-4. Comparison of the recoil mass distributions for different track resolutions after selection are shown in FIG. 5. It's apparent that the recoil mass spectra are quite similar for improved momentum resolution.

To quantify reconstruction resolution, the raw recoil mass is fitted by a single Gaussian distribution; the resulting fitted standard deviation is plotted in FIG. 6 as function of scale factors of track resolution parameters, it's obtained from fast MC produced by Pandora V2.1. Not surprisingly, the raw recoil mass resolution is sensitive to track momentum magnitude resolution, but not to track angular resolution. Hence the SD detector gives a narrower distribution than the LD detector. It should be noted, however, that initial state radiation and beamstrahlung leads to a highly asymmetric resolution function, poorly approximated by a Gaussian function.

Considering the effect of beam energy spread in Pandora V2.2, we redo the analysis which considers backgrounds from WW & ZZ. It turns out that recoil mass resolution is only sensitive to degraded track momentum resolution but less sensitive to improved ones, shown in FIG. 7. Here, two baseline detectors are simulated for fast MC events produced by Pandora V2.2 assuming $\sqrt{s} = 350$ and 500 GeV with Higgs masses at 120, 140 and 160 GeV. For the uncertainty of Higgs mass, it's shown in FIG. 8. What's more, we also use full simulation MC to determine the Z recoil mass resolution and accuracy shown in in FIG. 9 and FIG. 10, respectively. Clearly, the resolution and accuracy of Z recoil mass from full MC is worse than that from fast MC because of its worse track momentum resolution. A little better recoil mass resolution and precision derived from SD owes to somewhat better momentum resolution at large transverse track momentum $P_t > 10$ GeV.

Hence to quantify better the effect on final derived Higgs mass and cross section of track resolution parameters, a resolution-model-independent Monte Carlo interpolation fit method [7, 8] was used. The results are shown in FIG. 11 where it is confirmed that the Higgs mass determination is indeed sensitive to degraded track resolution for the parameters of 2001 North American baseline detector designs, while the production cross section determination is not. Consequently, the measurement of absolute values of Higgs branching ratios for a low-mass Higgs particle does not significantly influence the choice of tracking detector design at a linear collider. On the other hand, if one improves nominal momentum resolution by factor of 2 or more, the resolution and

precision of Z recoil mass won't gain too much. However, physics potential might be digged out by decreasing beam energy spread since better performance is seen for no beam energy spread case.

Future studies will include incorporation of measured jets from hadronic Higgs decay with a kinematic fit.

Acknowledgments

We wish to thank Michael E. Peskin, Masako Iwasaki, Gary Bower, Tony Johnson, Mike Ronan, Wolfgang Wolkowiak, Bruce A. Schumm, Rick van Kooten, John Jaros and Norman Graf, for kind help and many constructive discussions. This work is supported by the National Science Foundation of the United States under grant PHY-9984997.

-
- [1] B. Schumm (2001), snowmass 2001 proceedings.
 - [2] M. E. Peskin (1999), see also, <http://www-sldnt.slac.stanford.edu/nld/new/Docs/Generators/PANDORA.htm>, hep-ph/9910519.
 - [3] T. Sjostrand, *Comp. Phys Comm.* **82**, 74 (1994).
 - [4] T. Johnson, *Proceedings of the Inter. Conf. on Comp. in High Energy Physics (CHEP 98)* (1998), SLAC-PUB-7963.
 - [5] T. Abe et al. (American Linear Collider Working Group) (2001), resource book for Snowmass 2001, Colorado.
 - [6] L. C. Tracking-Group (2001), see http://www-mhp.physics.lsa.umich.edu/~keithr/LC/baselines_mar01.html.
 - [7] H. J. Yang and K. Riles (2001), snowmass 2001 proceedings.
 - [8] H. J. Yang and K. Riles (2002), at UC Santa Cruz Retreat talks.

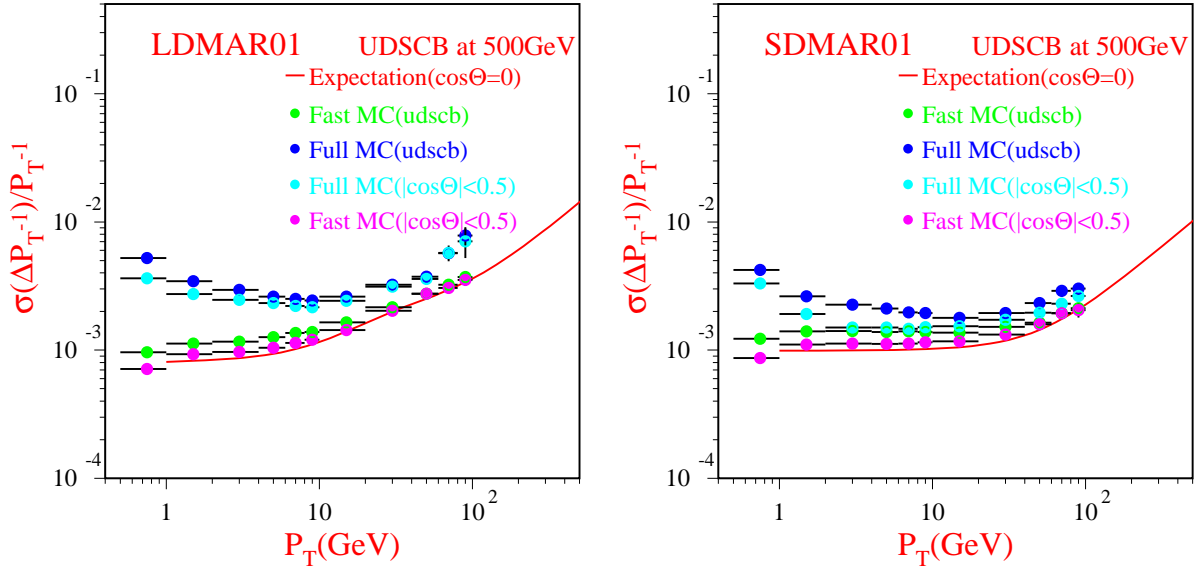


FIG. 1: Left – the track momentum resolution from the large detector plotted vs transverse track momentum. The red curve shows the expected momentum resolution for a track with $\cos\theta = 0$; the green and blue points show resolutions from fast MC and full detector simulation MC for $|\cos\theta| < 0.9$, respectively. The magenta and cyan points show the same for $|\cos\theta| < 0.5$. Right – corresponding results for the SD detector.

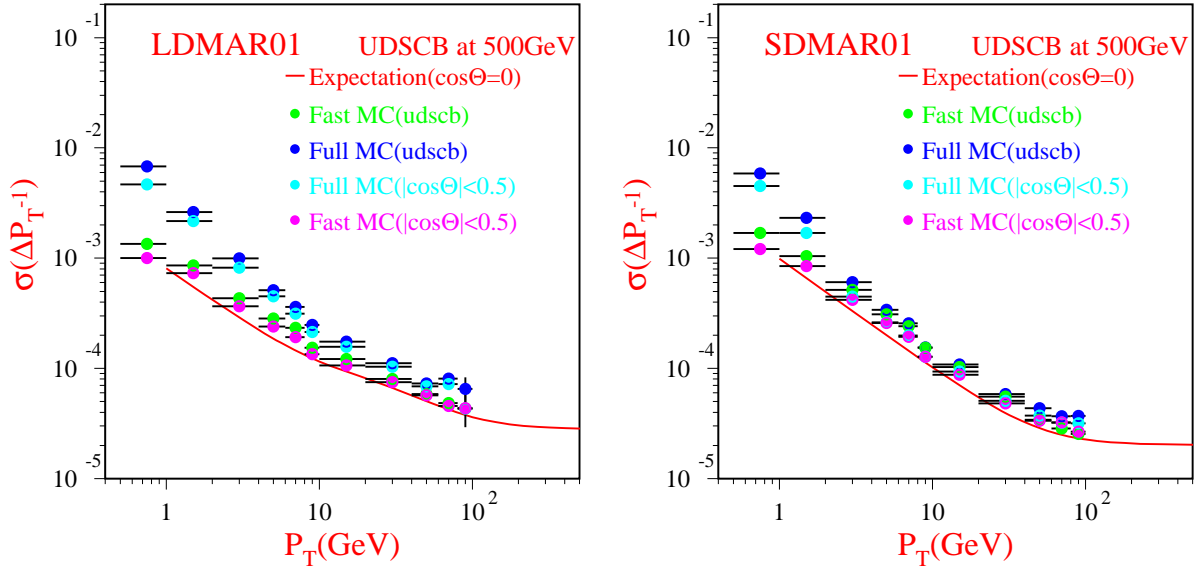


FIG. 2: Left – the track fractional momentum resolution from the large detector plotted vs transverse track momentum. The red curve shows the expected momentum resolution for a track with $\cos\theta = 0$; the green and blue points show resolutions from fast MC and full detector simulation MC for $|\cos\theta| < 0.9$, respectively. The magenta and cyan points show the same for $|\cos\theta| < 0.5$. Right – corresponding results for the SD detector.

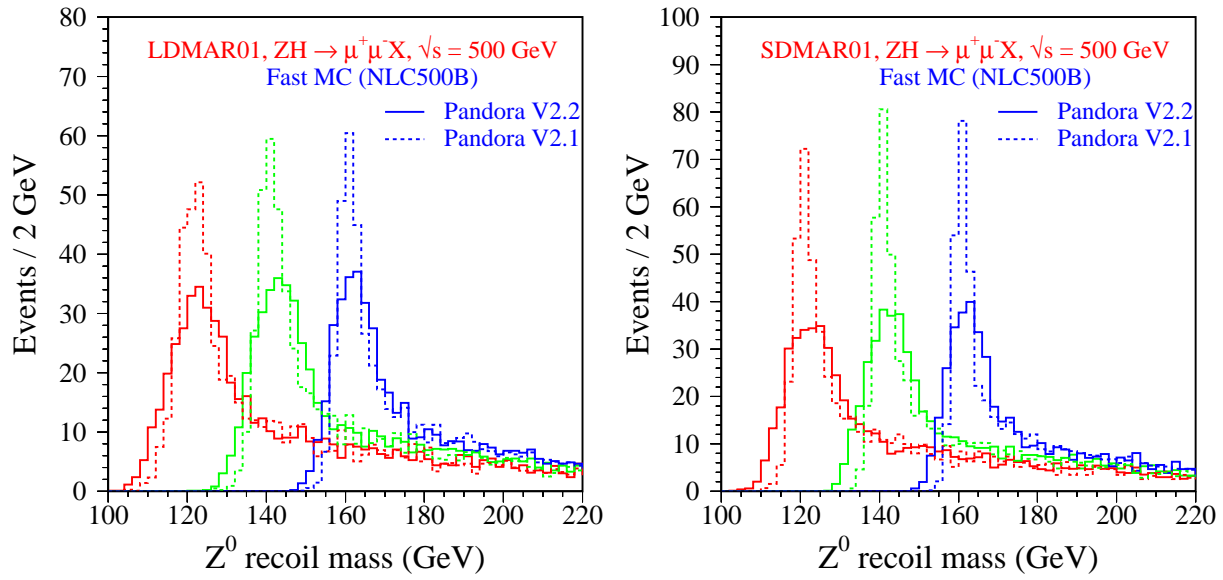


FIG. 3: Left – comparison of Z recoil mass distributions of $e^+e^- \rightarrow ZH \rightarrow \mu^+\mu^-X$ from fast MC for $\sqrt{s} = 500$ GeV and Higgs masses at 120(red), 140(green) and 160(blue) GeV, which are produced by Pandora V2.2(solid lines) and V2.1(dotted lines) and simulated by large detector. Right – the corresponding recoil mass distributions for silicon detector.

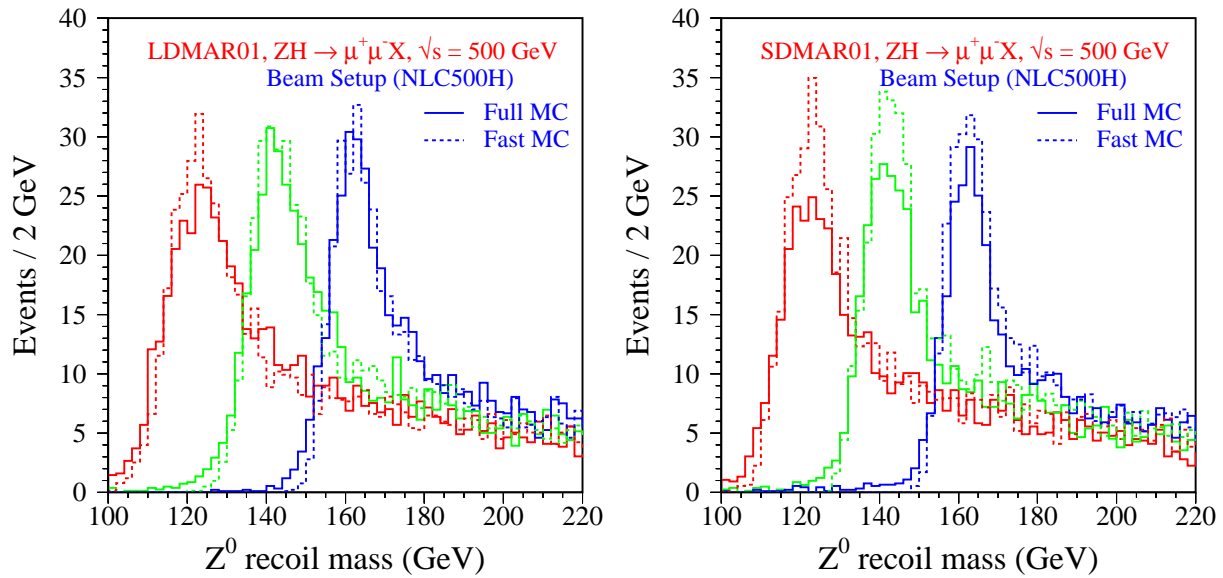


FIG. 4: Left – comparison of Z recoil mass distributions of $e^+e^- \rightarrow ZH \rightarrow \mu^+\mu^-X$ from fast and full MC for $\sqrt{s} = 500$ GeV and Higgs masses at 120(red), 140(green) and 160(blue) GeV, which are produced by Pandora V2.2 and simulated by large detector. Right – the corresponding recoil mass distributions for silicon detector.

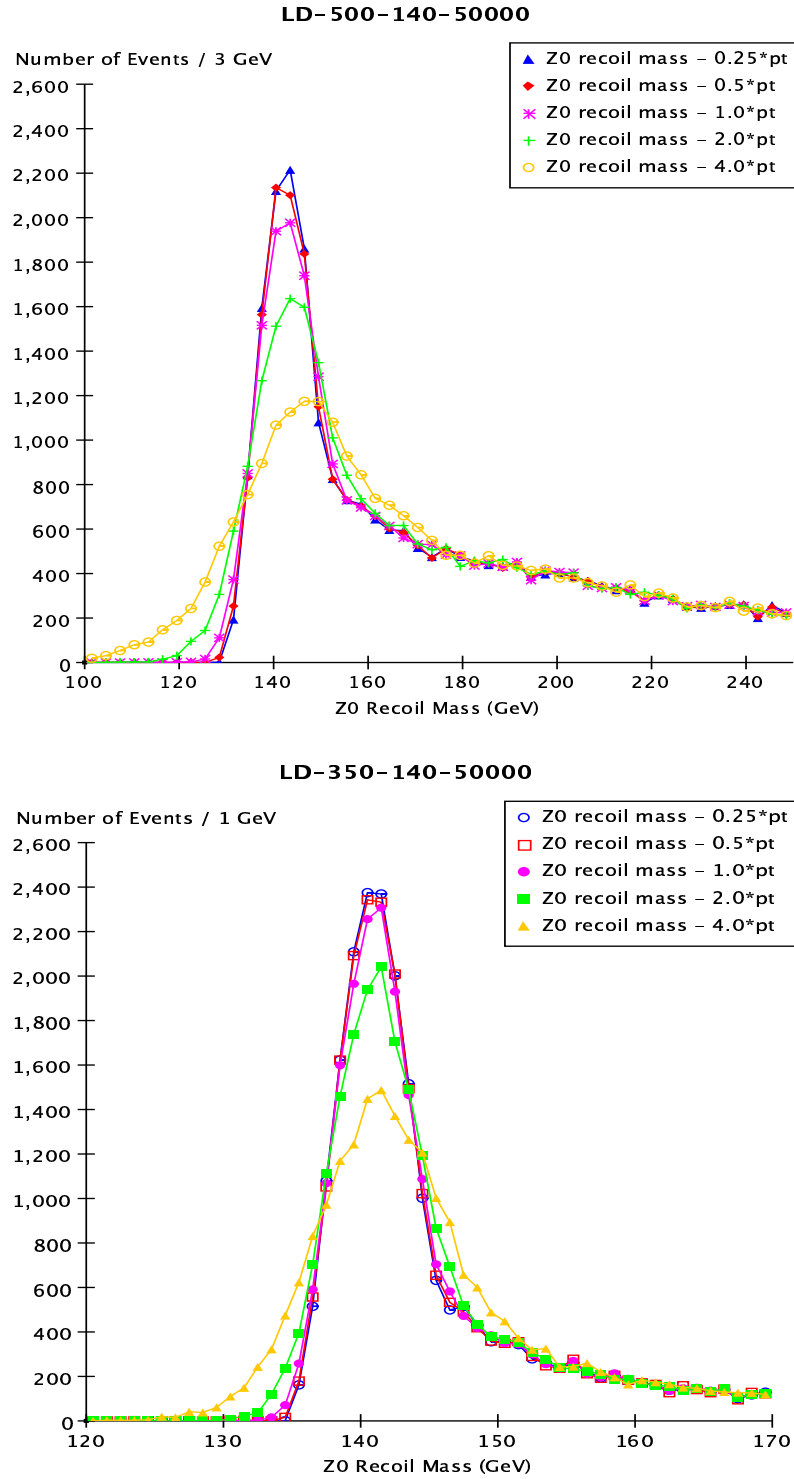


FIG. 5: Comparison of Z recoil mass distributions of $e^+e^- \rightarrow ZH \rightarrow \mu^+\mu^- X$ for various track momentum resolution scale factors, assuming $\sqrt{s} = 500$ GeV (top) and 350 GeV (bottom) with Higgs mass at 140 GeV.

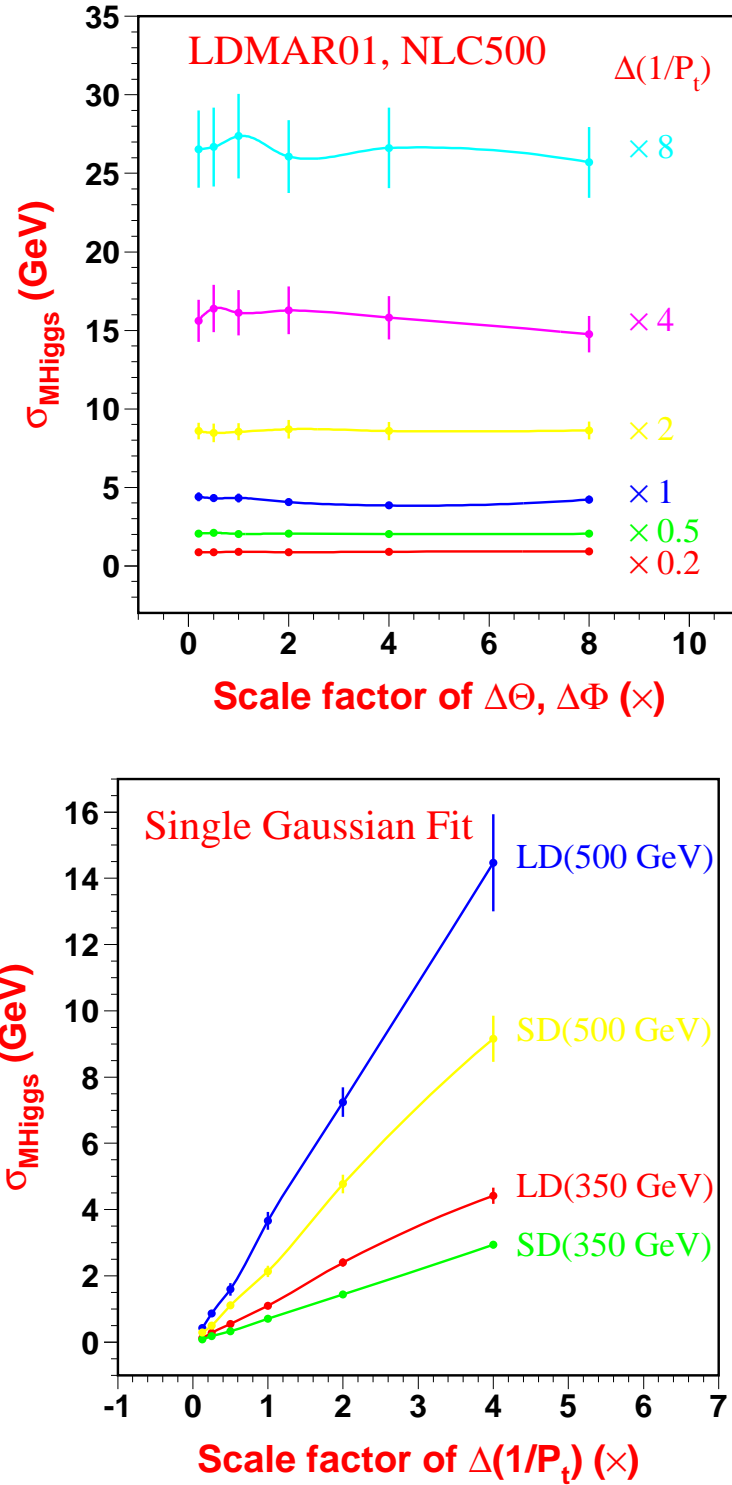


FIG. 6: Raw recoil mass resolutions from Pandora V2.1. Top – raw recoil mass resolutions for various angular resolution scale factors, assuming $\sqrt{s} = 500$ GeV with large detector. Bottom – raw recoil mass resolutions for various momentum magnitude resolution scale factors, where red and blue points correspond to the LD design at 350 GeV and 500 GeV, respectively. The green and yellow points correspond to the SD design.

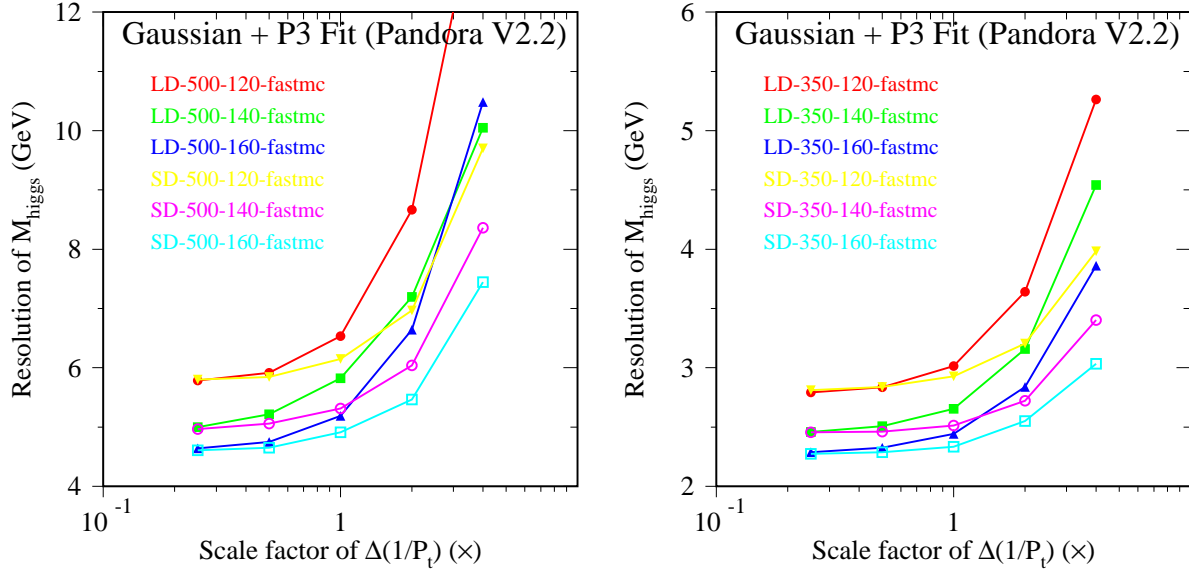


FIG. 7: Recoil mass resolutions for various track momentum resolution scale factors. Here, two baseline detectors are simulated for fast MC events produced by Pandora V2.2, assuming $\sqrt{s} = 500$ GeV(Left) and 350 GeV(Right) with Higgs masses at 120, 140 and 160 GeV.

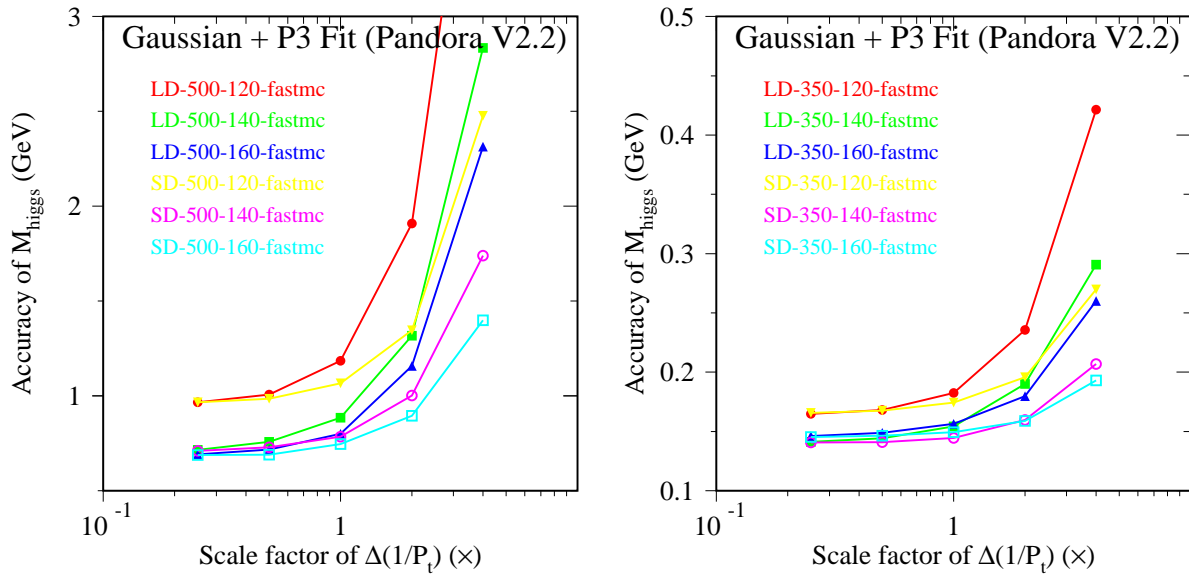


FIG. 8: Uncertainties of recoil mass for various track momentum resolution scale factors. Here, two baseline detectors are simulated for fast MC events produced by Pandora V2.2, assuming $\sqrt{s} = 500$ GeV(Left) and 350 GeV(Right) with Higgs masses at 120, 140 and 160 GeV.

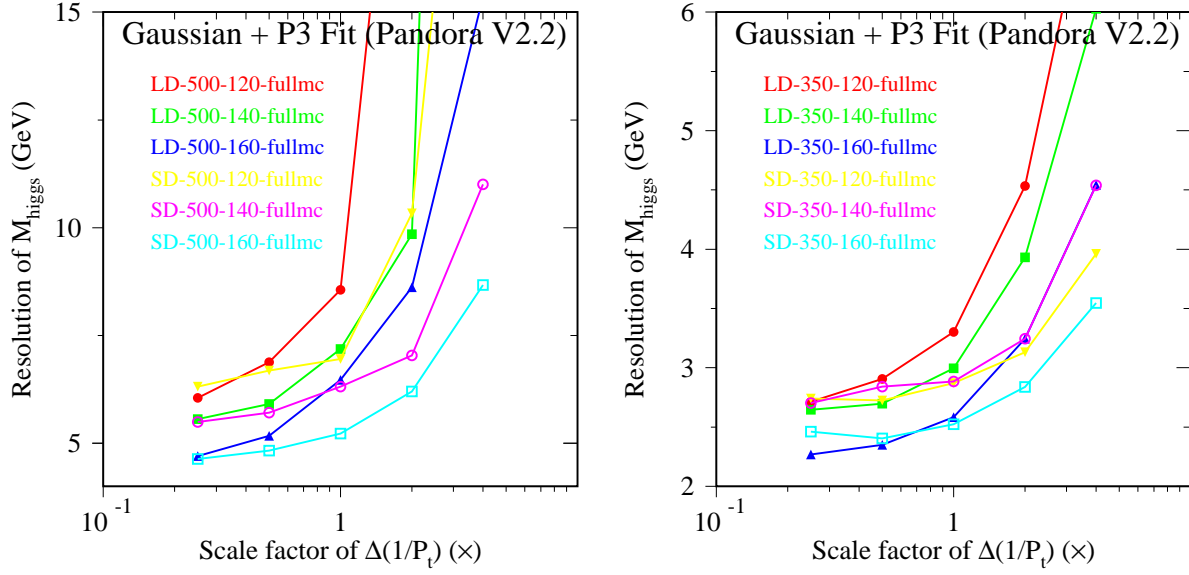


FIG. 9: Recoil mass resolutions for various track momentum resolution scale factors. Here, two baseline detectors are simulated for full MC events produced by Pandora V2.2, assuming $\sqrt{s} = 500$ GeV(Left) and 350 GeV(Right) with Higgs masses at 120, 140 and 160 GeV.

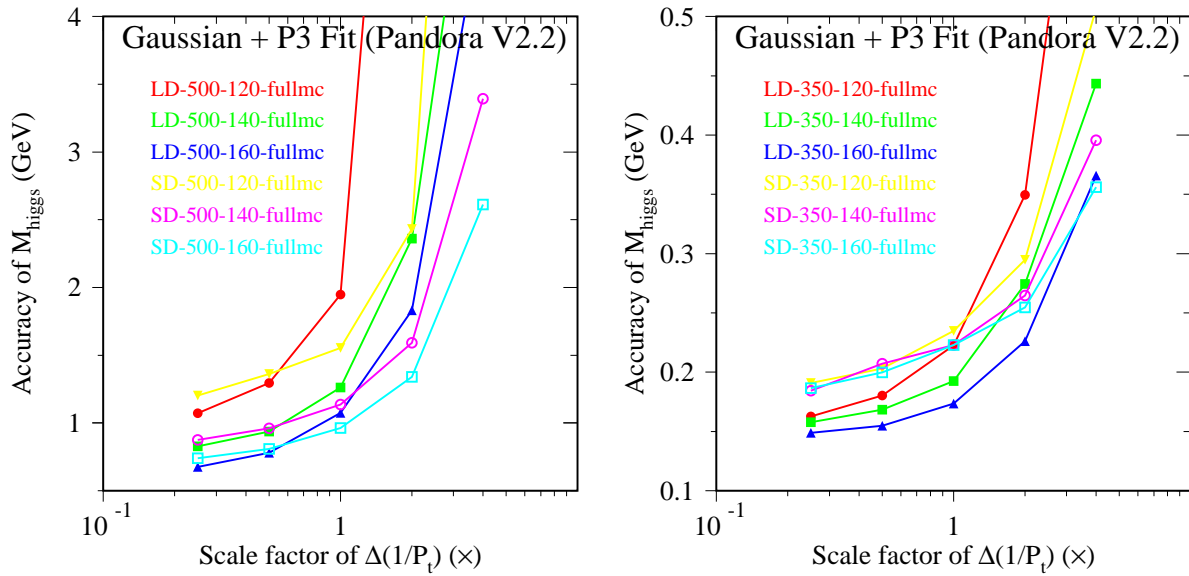


FIG. 10: Uncertainties of recoil mass for various track momentum resolution scale factors. Here, two baseline detectors are simulated for full MC events produced by Pandora V2.2, assuming $\sqrt{s} = 500$ GeV(Left) and 350 GeV(Right) with Higgs masses at 120, 140 and 160 GeV.

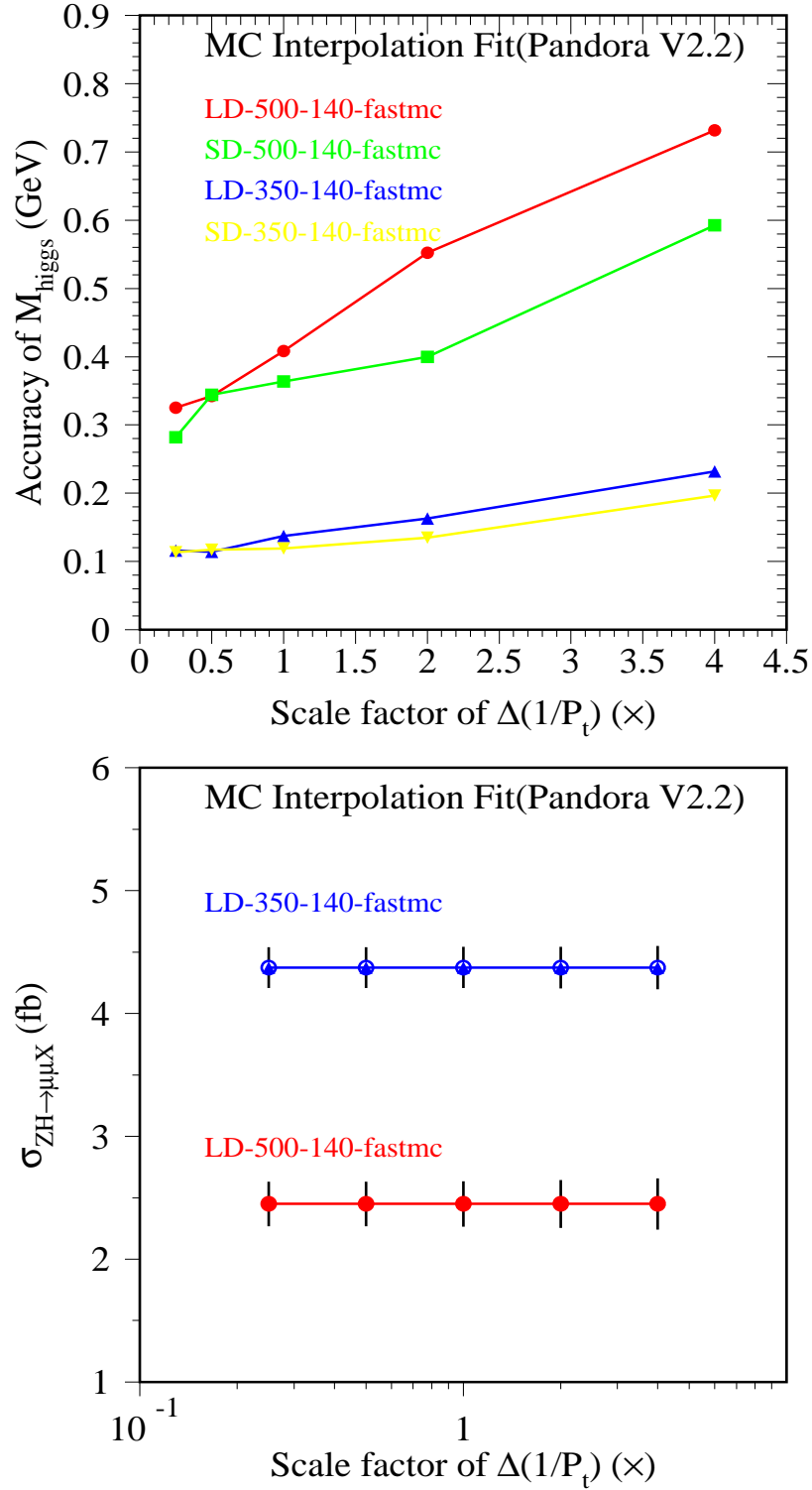


FIG. 11: Top– Accuracies of recoil mass for various track momentum resolution scale factors between 0.25 and 4. Bottom – Cross sections of $e^+e^- \rightarrow ZH \rightarrow \mu^+\mu^- X$ as function of track momentum resolution scale factors. Here two baseline detectors are simulated for fast MC events produced by Pandora V2.2, assuming $\sqrt{s} = 500$ GeV and 350 GeV with Higgs masses at 140 GeV.